NeuroImage 244 (2021) 118608

Contents lists available at ScienceDirect

NeuroImage

journal homepage: www.elsevier.com/locate/neuroimage

Early cortical signals in visual stimulus detection

Hunki Kwon[a], Sharif I. Kronemer[a,b], Kate L. Christison-Lagay[a], Aya Khalaf[a,f], Jiajia Li[a,e], Julia Z Ding[a], Noah C Freedman[a], Hal Blumenfeld[a,c,d,*]

[a] Department of Neurology, Yale University School of Medicine, 333 Cedar Street, New Haven, CT 06520-8018, USA
[b] Interdepartmental Neuroscience Program, Yale University School of Medicine, 333 Cedar Street, New Haven, CT 06520, USA
[c] Neuroscience, Yale University School of Medicine, 333 Cedar Street, New Haven, CT 06520, USA
[d] Neurosurgery, Yale University School of Medicine, 333 Cedar Street, New Haven, Connecticut 06520, USA
[e] School of Information and Control Engineering, Xian University of Architecture and Technology, Xi'an 710055, China
[f] Biomedical Engineering and Systems, Faculty of Engineering, Cairo University, Giza, Egypt

ARTICLE INFO

Keywords:
Intracranial EEG
Detection
Visual perception
Broadband gamma
Consciousness

ABSTRACT

During visual conscious perception, the earliest responses linked to signal detection are little known. The current study aims to reveal the cortical neural activity changes in the earliest stages of conscious perception using recordings from intracranial electrodes. Epilepsy patients (N=158) were recruited from a multi-center collaboration and completed a visual word recall task. Broadband gamma activity (40–115Hz) was extracted with a band-pass filter and gamma power was calculated across subjects on a common brain surface. Our results show early gamma power increases within 0-50ms after stimulus onset in bilateral visual processing cortex, right frontal cortex (frontal eye fields, ventral medial/frontopolar, orbital frontal) and bilateral medial temporal cortex regardless of whether the word was later recalled. At the same early times, decreases were seen in the left rostral middle frontal gyrus. At later times after stimulus onset, gamma power changes developed in multiple cortical regions. These included sustained changes in visual and other association cortical networks, and transient decreases in the default mode network most prominently at 300–650ms. In agreement with prior work in this verbal memory task, we also saw greater increases in visual and medial temporal regions as well as prominent later (> 300ms) increases in left hemisphere language areas for recalled versus not recalled stimuli. These results suggest an early signal detection network in the frontal, medial temporal, and visual cortex is engaged at the earliest stages of conscious visual perception.

1. Introduction

Sensory organs are the access points to self and the environment. While the structure of sensory organs and the character of its receptors filter sensory information to only a fraction of those available inputs, what remains is an overwhelming barrage of electrophysiological signals. The central nervous system has the challenging task of sorting through the avalanche of incoming multimodal signals, sifting through -irrelevant inputs and electrophysiologic noise for salient content. The initial stage in this critical process is signal detection. The goal of signal detection is to identify target inputs at the earliest stages of basic sensory decoding and propel those inputs for higher-order processing. The theoretical role of signal detection leads to several predictions about the spatial and temporal character of the detection network. First, signal detection should occur rapidly after sensory signal input. Speed is necessary for tasks with rigid temporal constraints. Signal detection as the first stage in a sequence of processing means that a delay in detection may decrease the detection rate as input signals decay or are masked by subsequent inputs, and may have downstream implications for subsequent higher-order processes. A second prediction is that the signal detection network should involve sensory cortex, as the earliest cortical processor for sensory signals, and particular networks in association cortices to offer flexibility in the definition of salience according to current goals, attention, and multimodal influences. Previous human and non-human primate studies on the earliest stages of signal input processing support these two major predictions on the spatiotemporal character of the detection network (Libedinsky and Livingstone, 2011; Thompson and Schall, 2000; Wang et al., 2018).

There is consensus that sensory cortices play a role in signal detection for those inputs that match their corresponding sensory modality. The temporal profile of sensory cortex matches the needs of signal detection by rapid access and early processing of sensory inputs. For example, the visual cortex is the earliest cortical structure to receive signal from the retina, with several studies showing signal arrival in visual cortex less

* Corresponding author at: Department of Neurology, Yale University School of Medicine, 333 Cedar Street, New Haven, CT 06520-8018, USA.
E-mail address: hal.blumenfeld@yale.edu (H. Blumenfeld).

https://doi.org/10.1016/j.neuroimage.2021.118608.
Received 13 June 2021; Received in revised form 19 August 2021; Accepted 20 September 2021
Available online 21 September 2021.

than 50ms post-stimulus (Deco and Lee, 2004; Fornaciai et al., 2017; Meeren et al., 2008; Schmolesky et al., 1998; Shigihara et al., 2016). Almost all visual information is first distributed to other cortical regions from primary visual cortex at the early stage of visual processing. Also, studies of visual perception show sensory regions are the first discriminating regions for perception within approximately 200ms post stimulus onset (Dobs et al., 2019; Gaillard et al., 2009; Herman et al., 2019; Li et al., 2019). These findings for early signaling in sensory cortex for vision are also reported in other modalities, including somatosensory and auditory stimuli (Meador et al., 2002; N'Diaye et al., 2004; Palva et al., 2005).

Long-range cortico-cortical and thalamo-cortical projections allow for rapid signaling between sensory and association cortices (Pennartz et al., 2019). Therefore, along with sensory cortex, association cortices can receive details of sensory signal early and guide signal detection. Likewise, the dorsal lateral prefrontal cortex is also among those consistently reported structures involved in early signal processing. For example, the frontal eye fields (FEF), traditionally associated with controlling eye movements and orienting, is also found engaged in signal detection (Bruce and Goldberg, 1985; Tehovnik et al., 2000). Neuronal activity in the FEF corresponds to visual perception and attention in macaque studies (Schall, 2002). Electrophysiological studies in monkeys suggest that neuronal responses in FEF increase at the earliest stage of visual perception, as early as 100ms post stimulus (Bichot and Schall, 2002; Bollimunta et al., 2018; Gregoriou et al., 2009; Thompson and Schall, 1999, 2000). Other evidence from animal models suggests that FEF neurons may have even earlier latencies, nearly as fast as primary visual cortex (Libedinsky and Livingstone, 2011; Petroni et al., 2001; Sommer and Wurtz, 2004). In human studies, FEF has shown cortical responses as early as 100ms post visual stimulus in scalp potential recordings (Foxe and Simpson, 2002). From intracranial EEG recordings in three patients with selective electrode coverage, FEF activity was found as early as 100ms post visual stimulus (Blanke et al., 1999). However, some human intracranial event-related potential studies have shown very fast responses in FEF as early as 24 - 45 ms after stimulus onset (Kirchner et al., 2009). In other human studies, transcranial magnetic stimulation (TMS) has been used to investigate the role of FEF during visual processing and a significant change in a time window of 40-80ms post stimulus in FEF is observed after presentation of the visual array (O'Shea et al., 2004). TMS over right FEF has been shown to disrupt performance on stimulus detection tasks (Grosbras and Paus, 2002). The FEF also plays an important role in connecting with and influencing other brain areas in the early stages of visual perception. Several studies have suggested that FEF is a major source of the attentional effects on frontal gamma frequency synchrony with visual cortex (Gregoriou et al., 2009) and the latency of FEF and temporal area spiking precedes visual cortex spiking (Schmolesky et al., 1998).

Beyond the FEF, several studies have suggested that prefrontal cortex and parietal cortex may be sources of top-down attentional control in the visual pathway (Gregoriou et al., 2009; Saalmann et al., 2007). The prefrontal cortex is the most likely origin of top-down facilitation in object recognition, and is activated directly from early visual areas to initiate top-down visual processing (Bar, 2003). Human brain imaging, including functional magnetic resonance imaging (fMRI) studies have further elucidated frontoparietal cortical networks involved in top-down attentional control, as well as subcortical-cortical networks crucial for bottom-up signal detection, although neuroimaging has lower time resolution than electrophysiological methods (Corbetta and Shulman, 2002; Dosenbach et al., 2007; Kinomura et al., 1996; Li et al., 2021; Seeley et al., 2007; Vossel et al., 2014). Outside the frontal lobes, neuronal activity in the parietal cortex is highly correlated with saccadic reaction time, suggesting that it has an important role in controlling of visual attention (Bisley and Goldberg, 2010). The activity of sampled neurons in the temporal area has also shown significant early changes identified by spike train analysis (Desimone and Duncan, 1995; Schmolesky et al., 1998). Neurons in the temporal lobe also respond shortly after the onset of visual stimuli and increase their firing rate in relation to visual awareness in monkeys and humans (Mormann et al., 2008; Wang et al., 2018). Previous findings on signal detection suggest a distributed network, temporally linked by rapid signaling. The ideal method for studying signal detection is a whole-brain recording approach with high temporal resolution, necessary to capture the rapid and transient detection electrophysiology. Intracranial EEG is the gold-standard for recording electrophysiological responses directly from the human brain with high spatiotemporal resolution (Baroni et al., 2017; Miller et al., 2014). By extracting changes in broadband gamma (40–115Hz) power, intracranial EEG can be used to infer the pattern of local changes in population neuronal activity (Li et al., 2019; Miller et al., 2014; Mukamel et al., 2005).

Therefore, the current study aims to elucidate the human visual detection network using recordings from intracranial electrodes implanted in a large number of patients that offers coverage of nearly the entire cortex for high temporal resolution electrophysiological recordings. We hypothesized based on prior work that this approach would provide unparalleled access to an early visual signal detection network including visual areas, frontal cortex and possibly other regions engaged at the earliest stages in conscious experience (Blumenfeld, 2021).

2. Materials and methods

2.1. Participants and subdural electrodes

A total of 158 participants (77 males; age range: 16-64 years old; mean ± std: 36.77 ± 11.38 years old) with drug-resistant epilepsy undergoing intracranial EEG implantation for seizure monitoring were recruited after written informed consent from all participants or their guardians. Among the participants, 131 were right-handed, 17 left-handed and 10 ambidextrous. Separate subgroup analyses of females and males did not show any major difference in results (see Supplementary Figs. S1, S2) so results were combined across sex. Similarly, separate analysis of right-handed individuals alone produced similar results to the overall cohort, and sample sizes for left-handed or ambidextrous individuals were too small to produce statistically significant results (data not shown), so analyses were combined across handedness to increase sample size. Participants were recruited from the neurology and neurosurgery departments of Boston Children's Hospital, Columbia University Hospital, Dartmouth Hitchcock Medical Center, Emory University Hospital, Freiburg University Hospital, Thomas Jefferson University Hospital, Mayo Clinic, National Institutes of Health, University of Texas Southwestern Medical Center and Hospital of the University of Pennsylvania. All research was conducted in accordance with the Declaration of Helsinki and under research protocols approved by the institutional review board at each recruitment site.

Electrodes included a combination of subdural strip, grid, and depth electrode contacts implanted according to recommendation of the clinical team to best localize epileptogenic regions. The EEG data were re-referenced to a bipolar montage and all data are presented as differential results for adjacent electrode pairs (Burke et al., 2013). Across all participants there were 14,860 intracranial electrode pairs (8382 left hemispheric and 6478 right hemispheric), after excluding 1797 electrode pairs in white matter or determined poor from its noise profile by the monitoring clinical team (Fig. 1B). Each participant was implanted with on average 94.05 ± 30.78 electrode pairs. These data may be publicly accessed at the Cognitive Electrophysiology Data Portal (http://memory.psych.upenn.edu/Electrophysiological_Data).

2.2. Free-recall task

Participants were instructed to complete a free-recall task, explained in previous publications (Burke et al., 2013; Long et al., 2014). The free-recall task involved three discrete task phases. First, participants

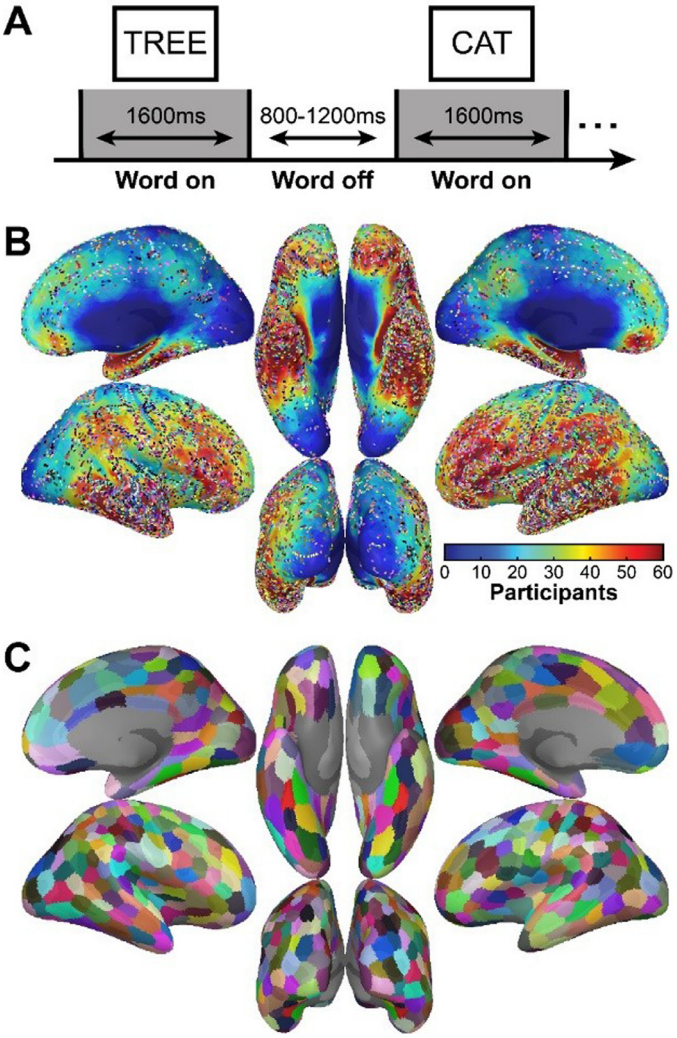

Fig. 1. Free Recall Task, electrode distribution, and parcellation map. **(A)** Participants completed a free recall task. A list of capital English words (*N*=15 or 20) were presented for 1600ms at 800–1200 ms intervals. After a distraction period (arithmetic problems lasting approximately 20 s), participants were instructed to verbally recall any words presented in the preceding task phase. **(B)** Density map of electrode distribution across subjects. All included electrodes pairs (*N*=14,860) from 158 participants in the study were mapped. Colored dots represent electrode pair midpoints, with a different color for each subject. Density map shows number of participants contributing to signal for each location on the brain surface, using a 15 mm radius analysis region centered on each electrode pair (see Methods for details). **(C)** 400-region bilateral parcellation map in FreeSurfer space (Schaefer et al., 2018) was used for regional correspondence across participants and cluster-based permutation testing.

were asked at their bedside to study a list of 12 capitalized, English nouns (e.g., TREE and CAT) in white letters on a black background displayed on a 15 inch Macbook computer monitor (approximate viewing angle of each word was 3 × 9 degrees). Words were chosen from a pool of high-frequency nouns without replacement (http://memory.psych.upenn.edu/WordPools). Each word was present for 1600ms, followed by a blank interstimulus period of a random interval between 800–1200ms (Fig. 1A). This temporal jitter served to anticorrelate the expectation or anticipatory physiological responses with successive word presentations (Sederberg et al., 2007). Because of the long presentation of fully opaque words, all stimuli are considered to have been perceived. Immediately following the word presentation phase, participants were asked to complete a series of self-paced, arithmetic problems until 20 s had elapsed since the preceding letter presentation phase (average duration of distraction task ~22 s, as participants were allowed to complete the current arithmetic problem when 20 s had elapsed). The goal of the distractor task was to reduce recall bias for the end-of-list words (Howard and Kahana, 1999). Finally, participants were instructed to verbally recall as many words shown in the initial word presentation phase as possible within 45 s. 25 word lists with 12 words each (300 nouns total) were used per session, and participants participated in two sessions on average (range 1–4). The average number of word presentations across all participants was 538.3 ± 27.6 (Mean ± SD). Task words were categorized as recalled (the participant correctly stated the previously presented word during the recall phase, 25.1 ± 0.8% (Mean ± SD) of total word presentations) or not recalled (the participant neglected the previously presented word). Subsequent analyses considered both recalled and not recalled words together (Recalled + Not Recalled) and in contrast (Recalled - Not Recalled).

2.3. Intracranial EEG recordings and localization

Depending on the study site, intracranial EEG data was recorded using a Bio-Logic, DeltaMed, Nicolet, GrassTelefactor, or Nihon Kohden EEG system. The signals were sampled at 500, 512, 1000, 1024, or 2000 Hz. For uniform analyses across sites, EEG signals sampled with a frequency above 500 Hz were downsampled to 500 Hz using the gete_ms.m function in EEG Toolbox (http://memory.psych.upenn.edu/Software). For temporal synchronization of electrophysiological recordings with actual word presentation on the screen, the experimental computer sent pulses through a parallel port via an optical isolator into an unused recording channel or digital input on the amplifier. These pulses aligned the clock of the experimental computer with the intracranial EEG recording system to a precision within the lowest sampling rate of the intracranial EEG recording (< 2ms) (Sederberg et al., 2007). As described previously (Burke et al., 2013; Long et al., 2014), electrode contact localization was achieved by co-registering the post-op CTs with the post-op MRIs using Brain Extraction Tool (BET) and FMRIB's Linear Image Registration Tool (FLIRT) in FMRIB Software Library (FSL) program (www.fmrib.ox.ac.uk/fsl) and mapped to the fsaverage brain surface in FreeSurfer space (https://surfer.nmr.mgh.harvard.edu/) after surface-based registration for each participant. The EEG data were re-referenced to a bipolar montage using adjacent electrode contact pairs (Burke et al., 2013), and the location of each electrode pair was represented by their Euclidian midpoint (Fig. 1B). Electrode pairs are referred to simply as electrodes below.

2.4. Intracranial EEG artifact rejection

Any electrodes defined by the clinical team as coming from brain lesions, broken leads or containing epileptic activity were excluded from the analysis. All remaining EEG data were then preprocessed using an in-house four-stage artifact rejection pipeline detailed previously (Herman et al., 2019; Li et al., 2019). The interval of interest for each trial was defined as lasting 2500ms, from 500ms pre- to 2000ms post-onset of word presentation. All artifact rejection stages were applied to all trials within each subject and each electrode regardless of whether they were Recalled or Not Recalled trials. The staged preprocessing procedure first involved calculating the power spectrum by Welch's power spectral density estimate function in MATLAB 2019b (www.mathworks.com). To remove trials with high frequency noise, including electrical line noise, any trial with a topographical prominence >200 μV/Hz in a frequency peak above 30 Hz was rejected. Next, any trial with the mean-square error (MSE) relative to zero < 200 μV^2 was rejected to remove low amplitude signals resulting from loose or unplugged electrodes. Third, the MSE relative to the mean voltage time course of remaining trials from the first and second preprocessing step was calculated and then any trial with a MSE value >3000 μV^2 was rejected to remove signals which had larger amplitude than normal. To avoid removing too many trials by this step, only the worst 20% of trials

were rejected for an electrode if the number of trials with MSE >3000 μV^2 exceeded 20% of trials. Finally, trials were rejected for a particular electrode if it contained any values beyond 5 standard deviations from the mean at any time point. The entire preprocessing pipeline rejected 19.81% ± 5.34% (mean ± std) of all trials across electrodes and participants.

2.5. Broadband z-score gamma power extraction

Broadband gamma power (40-115 Hz), a measure of population neuronal activity, was extracted for further analysis in this study. The approach for gamma power extraction was adapted from previous studies (Herman et al., 2019; Li et al., 2019). First, downsampled, preprocessed EEG trials were passed through a 40-115 Hz Butterworth band-pass filter (zero-phase, 40th order) using the filtfilt MATLAB function. When extracting broadband gamma, trials were 4500ms in duration that included a 1000ms buffer on both sides of each trial to eliminate filter edge effects. After filtering, the buffer period was removed and the final cut trials were 2500ms, including 500ms pre and 2000ms post word presentation onset. Gamma power was calculated by taking the square of the voltage output from the band-pass filter. To smooth the power responses over time, gamma power was averaged within 50ms windows with 25ms overlap, yielding a total of 98 windows across the entire 2500ms trial. Because temporal precision is important for this investigation, we tested the effects of our filtering and smoothing method on simulated data, and found that temporal smearing (leakage) between time windows was minimal (see Supplementary Fig. S3).

Next, one final artifact rejection measure was employed. Trials were rejected if the gamma power at any 50ms time window exceeded 20 SD of the mean across trials and 50 ms time windows for that electrode within each subject. The initial 19 windows (total time period: -500ms–0ms) correspond with the pre-stimulus or baseline period, and the subsequent 79 windows (total time period: 0ms to 2000ms) correspond with the post-stimulus period. Note that the -25–25ms time window was excluded by this definition. Finally, for each subject, z-scored gamma power was computed by taking the average of the baseline (-500ms–0ms) across all trials for each electrode, and using its mean and standard deviation to compute the z-score for every 50ms time point in each 2500ms trial. The z-score calculations were done across both Recalled and Not Recalled trials together. After z-scoring, subsequent analyses were performed either by grouping all stimuli together (Recalled + Not Recalled), or by subtracting data in these categories from each other (Recalled - Not Recalled). For each subject, Recalled + Not Recalled data were calculated by combining and averaging the z-scored gamma power timeseries across all trials within each electrode regardless of memory condition (Recalled or Not Recalled). For Recalled - Not Recalled analyses, z-scored gamma power timeseries were first averaged within stimuli categories for each electrode, and the difference of the electrode average z-scored gamma power was found between the Recalled and Not Recalled conditions.

2.6. Mapping z-scored gamma power to the brain surface

All participant electrodes were projected onto the fsaverage brain surface in FreeSurfer space and displayed on the inflated fsaverage brain surface (https://surfer.nmr.mgh.harvard.edu/) (Fig. 1B). The common brain surface was converted into a triangular mesh, and gamma power values were applied to vertices around each electrode using a distance criterion of 15mm radius sphere as described previously (Herman et al., 2019; Li et al., 2019). This process was done separately for the Recalled + Not Recalled and for the Recalled - Not Recalled data. In summary, first, electrode raw z-scored gamma power was assigned to vertices within 1mm radius sphere from that electrode. Next, electrode z-score gamma power was projected to vertices within a 1–15mm radius from the central vertex, but with a linearly descending gamma power gradient where a value of 0 was assigned to vertices at 15mm from the central vertex. Finally, all vertex-assigned z-scored gamma power values across electrodes were summed within each participant. This process was separately repeated for all 50ms time windows.

2.7. Statistical analyses

Due to the high number of subjects and electrodes in these data, standard statistical approaches are susceptible to false discoveries. Therefore, an adapted spatiotemporal cluster-based permutation test was applied to the z-scored gamma power for optimal identification of statistically significant changes in z-score gamma power compared to baseline and correction for multiple comparison. Implementing this statistical approach involved, first, subdividing the cortical brain vertex mesh into 400 non-overlapping regions (200 regions per hemisphere) utilizing a bilateral parcellation map (Fig. 1C) (Schaefer et al., 2018). Next, the spatial dimension of these data was reduced through conversion of vertices to parcels by assigning each vertex to one of the 400 possible parcels based on its location on the brain mesh. The z-scored gamma power of all vertices assigned to each parcel were averaged at each 50 ms time point within each participant. To obtain a cluster-based permutation distribution, we used a paired, two-tailed t-test across participants comparing mean z-scored gamma power of the pre-stimulus baseline and the pre- and post-stimulus period for all 400 parcels and all time points with an in-house MATLAB function modified from clust_perm1.m function in matlabmk Toolbox (http://kutaslab.ucsd.edu/matlabmk_fn_docs). This process was done separately for the Recalled + Not Recalled and for the Recalled - Not Recalled data. Baseline was calculated based on the mean of all trials prior to stimulus onset. A parcel and time point were considered eligible to join a cluster if the t-value fulfilled an alpha threshold of $p < 0.05$. All parcels and time points exceeding this threshold were clustered based on spatial and temporal adjacency (i.e., either spatially neighboring parcels or proximal time points). Summed t-values for each spatio-temporal cluster were then computed by taking the sum of the absolute value of t-values for all parcels and time points within each cluster. Positive and negative t-value clusters were defined separately, and the absolute value of their summed t-values were used for the permutation distribution function (below). The above procedure was repeated 2000 times. For each permutation, the gamma power z-score value at each parcel and time point was randomly shuffled with its paired baseline value across subjects. Finally, a permutation distribution was generated by taking the cluster with the largest absolute summed t-value for each permutation. Clusters in the unpermuted data were then considered significant if their absolute summed t-value exceeded the top 5% of the permutation distribution. As an additional step to avoid spurious brief clusters due to transient noise, we required any significant cluster to have a minimum duration of 150ms. To display results within significant clusters across subjects (see Figs. 2, 3), all vertex-assigned z-scored gamma power values were averaged across subjects and then, they were weighted by multiplying by the square root of the number of subjects contributing to each vertex. This weighting was intended to represent the improved signal/noise ratio (which scales by square root of sample size) expected for vertices with data from more patients, as described previously (Herman et al., 2019).

A similar procedure was used to determine statistical significance of gamma power changes in time courses generated for specific regions of interest (ROIs) (see next section; Figs. 4, 5). Z-scored gamma power values of the vertices within each ROI were averaged at each time point for each participant. The same cluster-based permutation testing method described above was applied, interchanging baseline and time points for each participant, but because only one region was considered, only temporal adjacency was used when defining clusters. Again, the cluster based statistical approach was applied to Recalled + Not Recalled and Recalled - Not Recalled data independently. Time courses of mean values within each ROI were displayed, with values for each vertex calculated as the average gamma power z-score across subjects weighted by multiplying by the square root of the number of subjects at each ver-

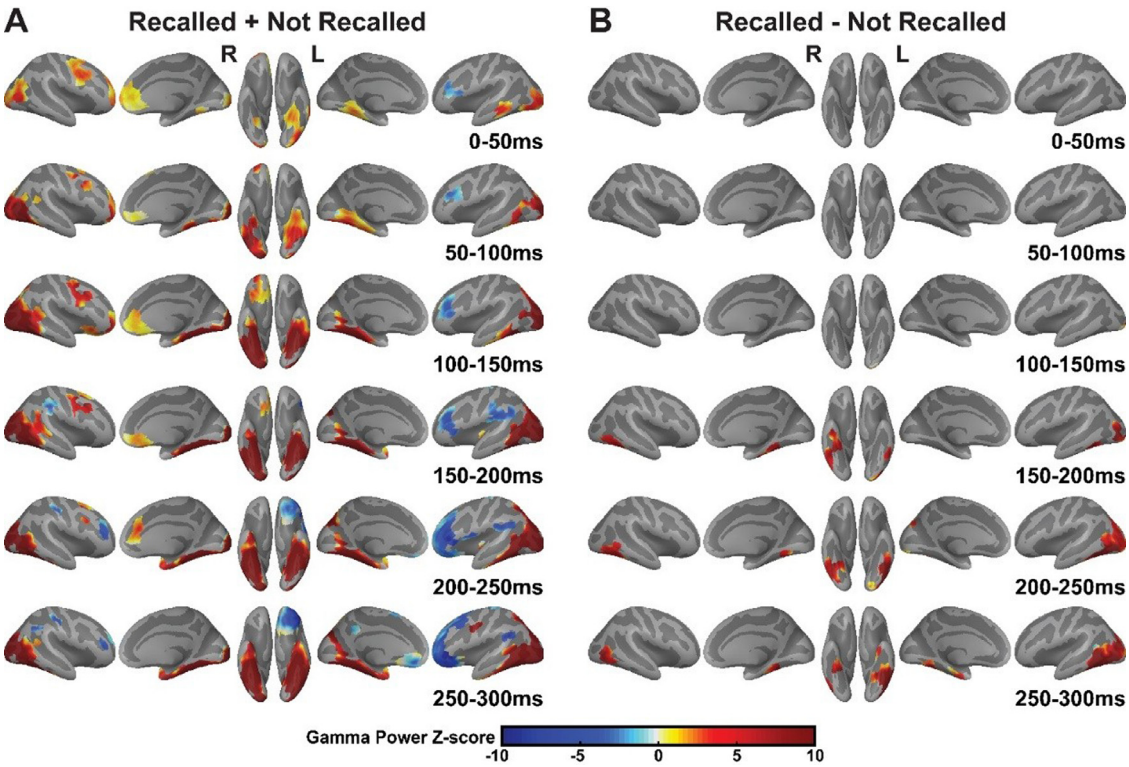

Fig. 2. Gamma power activity changes at the early stages of visual perception. Significant spatiotemporal gamma power (40–115 Hz) activity changes relative to baseline (500 to 0 ms before word presentation) were identified by cluster-based permutation testing ($p < 0.05$). **(A)** Based on all event trials regardless of whether the word was recalled, defined as Recalled + Not Recalled, gamma power increased at the earliest stage of word detection (0–150 ms) in bilateral lateral occipital and ventral fusiform visual association cortex, bilateral parahippocampal cortex, left posterior inferior temporal cortex, right dorsal-lateral frontal cortex (overlapping frontal eye fields), right ventral-medial and right orbital/ frontopolar cortices; and decreased in left dorsolateral frontal cortex. Later, gamma power increases and decreases were seen in multiple regions (150–300 ms, see text). **(B)** There were no significant gamma power differences for recalled versus not recalled stimuli, defined as Recalled - Not Recalled, at the earliest stage of word detection (0–150 ms). However, gamma power differences for Recalled - Not Recalled were seen lateral occipital and ventral fusiform visual association cortex at later times (150–300 ms). N=158 subjects. See also Supplementary PPT S1 and S2 for full detailed time course maps.

tex (Herman et al., 2019). Significant time points were then indicated on the time courses based on permutation statistics, where the absolute summed t-values of clusters exceeded the top 5% of the permutation distribution (see Figs. 4, 5).

2.8. Regions of Interest

To visualize gamma power changes among specific cortical anatomical areas, twelve anatomical regions of interest were identified from the Desikan-Killiany-Tourville (DKT) atlas in FreeSurfer (Klein and Tourville, 2012). These anatomical regions were divided into two groups according to their temporal character in whole-brain gamma power visualization: early and late stage regions of interest. The early stage regions (Fig. 4A) included lateral occipital cortex (LO), fusiform gyrus (FG), parahippocampal gyrus (PH), caudal middle frontal gyrus (CMF), orbitofrontal cortex (OFC) and ventral medial frontal cortex (VMF). The OFC ROI in this study corresponded to the lateral orbital frontal ROI from the DKT atlas; the VMF ROI in this study included both the medial orbital frontal and rostral anterior cingulate ROIs from the DKT atlas.

The late stage regions (Fig. 5A) included superior parietal cortex (SP), inferior parietal cortex (IP), superior frontal cortex (SF), inferior frontal cortex (IF), rostral middle frontal cortex (RMF) and inferior temporal cortex (IT). Pars opercularis, pars orbitalis, and pars triangularis from the DKT atlas were grouped to form our IF ROI. The supramarginal and inferior parietal ROIs from the DKT atlas (the latter corresponding more accurately to the angular gyrus) were combined to form our IP ROI. The middle temporal and inferior temporal ROIs from the DKT atlas were combined to form our IT ROI.

3. Results

3.1. Early cortical signal changes with visual stimuli

At the earliest times after stimulus presentation (0–150 ms), there were no significant differences between gamma power changes for Recalled versus Not Recalled stimuli (Fig. 2B, Recalled - Not Recalled). Therefore, we examined the combined Recalled and Not Recalled data for early cortical changes shared across trials (Fig. 2A, Recalled + Not Recalled). As expected, this revealed early changes in bilateral visual processing areas, including occipital cortex, and fusiform gyri, as well as the left posterior inferior temporal gyrus. Interestingly, changes also appeared as early as 0-50ms after stimulus onset in frontal cortical networks and in medial temporal regions (Fig. 2A). These included increases in the right caudal middle frontal gyrus (overlapping frontal eye fields), right ventral medial/frontopolar cortex, right orbital frontal cortex, and the bilateral medial temporal parahippocampal gyri (Fig. 2A). Early decreases were found in the left rostral middle frontal gyrus (Fig. 2A).

Time course analyses confirmed the observed early changes in visual, frontal and temporal cortical networks (see Fig. 4). In region of interest analyses, the earliest increases in cortical gamma activity were seen in the combined Recalled + Not Recalled data in the bilateral occipital, fusiform and medial temporal (parahippocampal) cortex, and in the right caudal middle frontal gyrus, right orbital frontal, and right

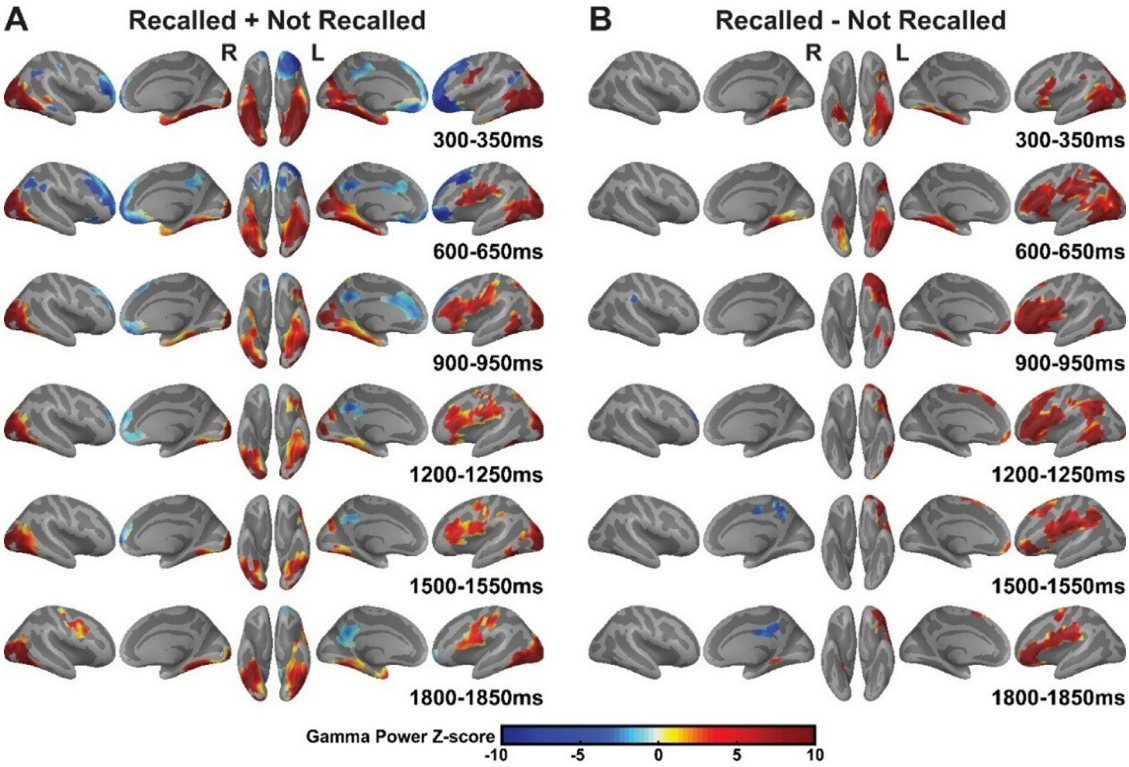

Fig. 3. Gamma power activity changes at the later stages of visual perception. The same statistical approach as Fig. 2 was applied (see Methods). **(A)** For Recalled + Not Recalled data, after early stages of word detection (> 300ms) gamma power increases continued in multiple brain areas; and decreases were seen in the default mode network as well as in other regions. **(B)** For Recalled - Not Recalled data, gamma power increases for recalled words were greater in the bilateral medial temporal cortex, and in multiple regions of left hemisphere language networks. *N*=158 subjects. See also Supplementary PPT S1 and S2 for full detailed time course maps.

ventral medial frontal cortex (see Fig. 4B). The early changes in the first 150 ms were significantly greater in the right hemisphere for the orbital and ventral medial frontal cortex (green bars in Fig. 4B). Overall, both the cortical surface maps and time course analyses show very early gamma activity increases within 0-50ms after stimulus onset in visual processing areas including bilateral occipital and fusiform cortex, in medial temporal parahippocampal gyri, and in the right frontal cortex.

3.2. Later cortical signal changes

Later gamma power changes > 150 ms after stimulus onset revealed a sequence of increases and decreases in multiple cortical regions (Figs. 2, 3). One set of changes was a continuation of the gamma power changes observed at earlier times in visual (lateral occipital and fusiform gyri), medial temporal and frontal cortical areas, which progressed and became more prominent at later times for the Recalled + Not Recalled stimuli (Figs. 2A and 3A). The early gamma power increases in lateral, medial and orbital frontal cortical networks gave way to later decreases at >300 ms in these same regions (Fig. 3A). In addition, gamma power decreases in default mode network areas were observed, including bilateral precuneus, posterior inferior parietal lobule, and ventral medial frontal cortex. These default mode network decreases appeared most prominently at approximately 300–650 ms after stimulus onset (Fig. 3A), as reported previously for consciously perceived visual stimuli (Herman et al., 2019).

As already noted, for Recalled - Not Recalled, there were no significant gamma power differences at the earliest stage of word detection (0–150 ms) (Fig. 2B). However, gamma power differences were present in bilateral occipital, fusiform cortex and some parts of the medial temporal cortex starting from intermediate stages (Fig. 2B, 150–300 ms) and continuing at later times (Fig. 3B, 300–650 ms). This suggests more activity was present in higher-order visual processing and memory networks for Recalled versus Not Recalled stimuli. In addition, at timepoints >300ms from word presentation, significant left hemispheric differences were observed in extensive frontal, parietal and temporal language regions for Recalled versus Not Recalled stimuli (Fig. 3B), similar to results reported previously for this verbal memory task (Burke et al., 2014). The full detailed time courses of changes for Recalled + Not Recalled and for Recalled – Not Recalled stimuli can be found in Supplementary PPT S1 and S2.

The region of interest time courses confirmed the findings shown in the whole brain cortical surface maps at later times (Figs. 4, 5). Persistent gamma power increases were seen in the Recalled + Not Recalled data for lateral occipital, fusiform, parahippocampal (Fig. 4B), superior parietal and inferior temporal cortices (Fig. 5B). At later times, decreases were seen in the Recalled + Not Recalled data in caudal middle frontal, orbital frontal, ventral medial frontal (Fig. 4B), superior frontal and rostral middle frontal cortices (Fig. 5B). In this verbal memory task, several regions showed significantly greater increases in the left hemisphere for Recalled + Not Recalled stimuli (green bars in Figs. 4B, 5B). When we compared Recalled - Not Recalled stimuli, in agreement with the brain maps, ROI analyses again showed significantly greater increases at later times (> 150ms) for Recalled stimuli in bilateral lateral occipital, fusiform and parahippocampal cortices (Fig. 4C). In addition, we again saw greater increases in left hemisphere language areas at later times (> 300ms) for Recalled - Not Recalled stimuli in the left orbital frontal, inferior parietal, superior frontal, inferior frontal, and rostral middle frontal cortices (times indicated by green bars in Figs. 4C, 5C).

4. Discussion

The current study examined the spatiotemporal neural activity changes at early and late stages of visual perception using recordings from intracranial electrodes implanted in large number of pa-

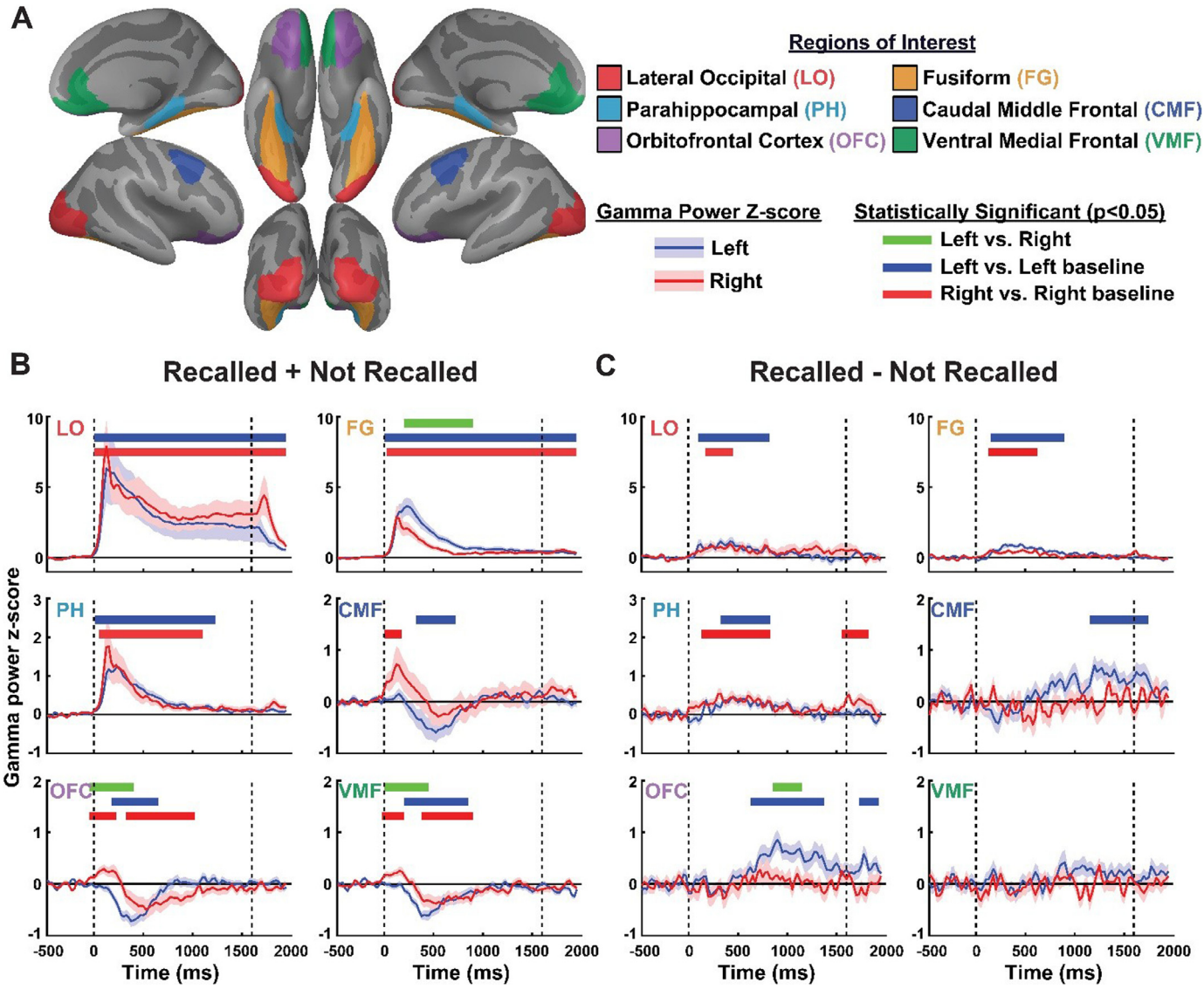

Fig. 4. Time course of gamma power in anatomical regions with early changes (0–150 ms) during visual perception. **(A)** Six different anatomical regions of interest were identified from a Desikan-Killiany-Tourville atlas in FreeSurfer (see Methods) showing changes at the early stages of visual perception (0–150 ms): lateral occipital cortex (LO), fusiform gyrus (FG), parahippocampal gyrus (PH), caudal middle frontal gyrus (CMF), orbitofrontal cortex (OFC) and ventral medial frontal cortex (VMF). **(B)** Recalled + Not Recalled data. LO, FG and PH in both hemispheres showed significant gamma power increases for about all of the time that words were presented. Right CMF, OFC and VMF also showed significant gamma power increases at the earliest times. Gamma power later decreased significantly in CMF, OFC and VMF. In FG, OFC and VMF, there were significant gamma power differences between the left and right hemisphere for < 500ms from word presentation. **(C)** Recalled - Not Recalled data. There were no significant differences between recalled and not recalled stimuli at the earliest stage of word detection. At times greater than ~100–150 ms, LO, FG and PH in both hemispheres showed significantly greater gamma power for recalled stimuli. At later times after word onset, left hemisphere CMF and OFC regions showed significantly greater gamma power for recalled stimuli. **(B,C)** Mean gamma power z-score time courses are shown (blue traces, left hemisphere; red traces, right hemisphere) ± standard error of mean (SEM) across subjects (blue or red shaded areas). Vertical dotted lines represent visual stimulus onset and offset. Thick horizontal bars indicate significant difference for gamma power in left versus right hemisphere (green bars), left hemisphere versus baseline (blue bars), or right hemisphere versus baseline (red bars) by permutation testing ($p < 0.05$). Baseline is defined as the 500 ms time period before word presentation. N=158 subjects (For interpretation of the references to color in this figure legend, the reader is referred to the web version of this article.).

tients. These distinct temporal windows correspond with signal detection (early) and signal processing/encoding (late), with the latter having implications for future recall of the stimulus. Broadly, the results showed very early (within 0-50ms of stimulus onset) gamma power increases in visual processing cortex, right frontal cortex, and medial temporal cortex. Together, these regions may work as a signal detection network for rapid visual input identification and initiation of processing. At later times after stimulus presentation, we observed sustained changes in visual and other association cortical networks, transient decreases in the default mode network, and prominent increases in medial temporal and left hemisphere language areas, which were greater for subsequently Recalled versus Not Recalled stimuli. These later changes observed when comparing Recalled versus Not Recalled stimuli suggest a possible role in the later dynamics of successful stimulus encoding.

4.1. Early stage signal detection

We observed that prefrontal areas showed gamma power significantly increased above baseline at the earliest stage of visual perception (Fig. 2A). In region of interest analyses, the caudal middle frontal cortex (including frontal eye fields), orbital frontal cortex and ventral medial/frontopolar cortex showed significant gamma power increases

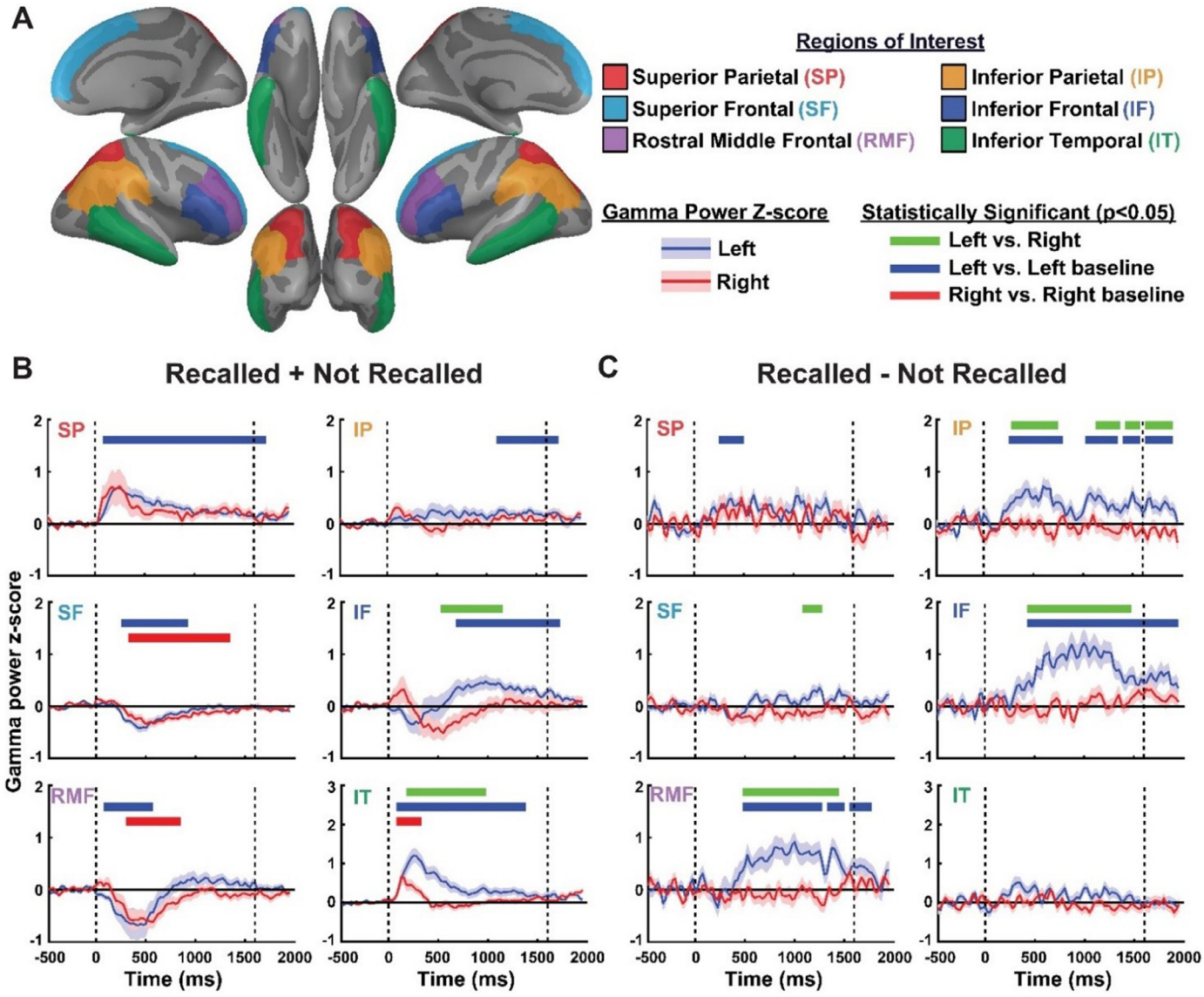

Fig.e 5. Time course of gamma power in anatomical regions with later changes during visual perception. **(A)** Six different anatomical regions of interest were identified from a Desikan-Killiany-Tourville atlas in FreeSurfer (see Methods) showing changes at the later stages of visual perception: superior parietal lobule (SP), inferior parietal lobule (IP), superior frontal gyrus (SF), inferior frontal gyrus (IF), rostral middle frontal gyrus (RMF) and inferior temporal cortex (IT). **(B)** Recalled + Not Recalled data. Persistent gamma power increases were seen in SP and IT. Decreases were seen in SF, IF and RMF. In this verbal memory encoding task, IF and IT showed significantly greater increases in the left hemisphere. **(C)** Recalled - Not Recalled data. There were significantly greater increases in the left hemisphere IP, SF, IF and RMF for recalled stimuli. **(B,C)** Mean gamma power z-score time courses are shown (blue traces, left hemisphere; red traces, right hemisphere) ± standard error of mean (SEM) across subjects (blue or red shaded areas). Vertical dotted lines represent visual stimulus onset and offset. Thick horizontal bars indicate significant difference for gamma power in left versus right hemisphere (green bars), left hemisphere versus baseline (blue bars), or right hemisphere versus baseline (red bars) by permutation testing ($p < 0.05$). Baseline is defined as the 500 ms time period before word presentation. N=158 subjects (For interpretation of the references to color in this figure legend, the reader is referred to the web version of this article.).

rapidly following stimulus presentation (Fig. 4B). These results correspond with macaque studies that show the neuronal activity in the prefrontal cortex, especially in the frontal eye fields, corresponds to visual perception and attention; neuronal responses in frontal eye fields have previously been shown to increase at the earliest stage of visual perception. Several studies have shown responses within 100 ms post-stimulus (Bichot and Schall, 2002; Bollimunta et al., 2018; Gregoriou et al., 2009; Thompson and Schall, 1999, 2000), although other work suggests that FEF neurons may have even earlier latencies, nearly as fast as primary visual cortex (Libedinsky and Livingstone, 2011; Petroni et al., 2001; Sommer and Wurtz, 2004). In human studies, a critical change in time window between 40-80ms post-stimulus in frontal eye fields is observed after presentation of a visual array, and the frontal eye fields also show cortical responses within 100 ms post visual stimulus (Blanke et al., 1999; Foxe and Simpson, 2002; Grosbras and Paus, 2002; Muggleton et al., 2003; O'Shea et al., 2004); and some human intracranial event-related potential recordings have shown very fast responses in FEF as early as 24–45 ms after stimulus onset (Kirchner et al., 2009). Our findings are consistent with previous studies, in which the prefrontal cortex, including the frontal eye fields, is considered an important early region for visual perception and attention (Gregoriou et al., 2009).

We observed asymmetrical neuronal changes in prefrontal cortex including frontal eye fields at the earliest stage of visual perception. Some previous work suggests that the right hemisphere may be dominant for bottom up attention capture and salience (Corbetta and Shulman, 2002; Shulman et al., 2010). We found that the right hemisphere

prefrontal cortex (caudal middle frontal, orbital frontal, ventral medial frontal/frontopolar cortex) showed significant gamma power increases which were not observed in left hemisphere at the earliest stage of visual perception (Figs. 2A, 4B). This finding corresponds with TMS studies that find specifically the right frontal eye fields influence attentional gamma power modulation in visual cortex (Duecker et al., 2013; Grosbras and Paus, 2002; Marshall et al., 2015; Silvanto et al., 2006). TMS of frontal eye fields in the right hemisphere also were shown to increase BOLD activity in visual processing during a TMS-fMRI study (Heinen et al., 2014). Our findings in the prefrontal cortex during intracranial EEG are consistent with previous studies suggesting that early visual signal detection and processing is largely lateralized to the right frontal eye fields. However, our results were not limited to frontal eye fields, but included a larger prefrontal cortical network. In addition to right caudal middle/frontal eye fields, we observed increases in right orbitofrontal and ventral medial/frontopolar cortex, as well as intriguing early gamma power decreases in the rostral middle frontal gyrus of the left hemisphere (Fig. 2A). The possible functional role of these broader bilateral frontal networks in early signal detection should be investigated further.

Beyond the neuronal activity changes in the prefrontal cortex, we observed significant very early gamma power increases in visual processing and medial temporal regions. The observed early changes in visual cortex, including the lateral occipital and ventral fusiform gyri are consistent with previous human and non-human primate work in visual stimulus detection (Herman et al., 2019; Schmolesky et al., 1998). Of note, the present study focused on lateral and ventral visual cortex because we had relatively sparse coverage in medial occipital regions (Fig. 1B), however prior human intracranial work has shown early increases in medial occipital cortex as well (Li et al., 2019). The lateral posterior inferior temporal cortical increases in gamma activity we observed at very early times, particularly on the left side (Fig. 2A), could also participate in early visual detection and processing, or might be part of basal temporal language networks given the verbal nature of the word encoding task (Benjamin et al., 2017; Luders et al., 1991). In a similar manner, the bilateral medial temporal parahippocampal increases we observed at very early times could be related to the specific mnemonic nature of the task, or could reflect a broader early role of medial temporal and hippocampal circuits in higher order association, context-dependence and relational aspects of stimulus processing (Hassabis et al., 2007; Konkel and Cohen, 2009; Schacter et al., 2007; Turk-Browne et al., 2009). In addition, recent work suggests that frontal and medial temporal circuits may interact in visual stimulus detection (Wang et al., 2018).

At slightly later times, but still within the first ~200 ms of stimulus onset, we observed gamma power increases in the superior parietal cortex (Figs. 2A, 4B). Numerous previous studies have demonstrated that the parietal cortex has an important role in visual perception and attention (Bisley and Goldberg, 2010; Critchley, 1962). Several studies have also suggested that parietal cortex may be a major source of top-down attentional feedback in the visual pathway, and thus an increase in neuronal activity might be helpful in early stages of visual perception (Bisley and Goldberg, 2010; Corbetta and Shulman, 2002; Gregoriou et al., 2009; Saalmann et al., 2007). This is further supported by early increases in the firing rate of neurons sampled from lateral temporal and parietal neocortical areas (Desimone and Duncan, 1995; Schmolesky et al., 1998). These activated regions may have interconnected functions that could enhance activity of neurons in visual cortex at the earliest stages of visual perception (Knudsen, 2011; Schall et al., 1995; Thompson and Schall, 2000).

We found no significant differences between activity elicited by Recalled and Not Recalled words at the very early stages of visual processing, within 150 ms of stimulus onset (Fig. 2B). At intermediate times beginning ~150 ms after stimulus onset, the earliest differences that we observed between Recalled and Not Recalled stimuli were larger gamma power increases for Recalled stimuli in the lateral occipital, fusiform and parahippocampal cortices (Figs. 2B, 4C). The findings in these regions may represent relatively early neural signatures that differentiate stimuli that are subsequently successfully recalled, in agreement with previous work (Burke et al., 2014).

4.2. Late stage signal processing and encoding

After early stages of visual perception, gamma power increases persist in the visual, frontal and medial temporal cortex during the later stages of visual stimulus presentation, suggesting some parts of the detection network are still activated for later higher-order processing. We also observed later decreases in gamma power in default mode network regions following stimulus presentation, consistent with previous intracranial EEG studies (Dastjerdi et al., 2011; Foster et al., 2012; Herman et al., 2019; Jerbi et al., 2010; Li et al., 2019; Miller et al., 2009; Ossandón et al., 2011; Ramot et al., 2012). In addition, at later times > 300 ms after word stimulus presentation, we observed significant left hemispheric differences in extensive frontal, parietal and temporal language regions for Recalled versus Not Recalled stimuli. These included greater increases for Recalled word stimuli in the left orbital frontal, inferior parietal, superior frontal, inferior frontal, and rostral middle frontal cortices. It has been proposed that these late language network changes are related to encoding of the verbal memory stimuli, as reported previously for this task (Burke et al., 2014). These regions are largely non-overlapping with the earliest responses, suggesting that the networks involved in early detection and late encoding are unique and separate.

4.3. Limitations

Intracranial EEG offers unparalleled access to human brain electrophysiology, yet is limited by the heterogeneous electrode coverage dictated by the clinical needs of the patient. While the current study's large sample size offered full brain coverage, electrode placement was densest on the lateral surfaces and sparser on the medial surface. Therefore, it is harder to interpret results involving those regions where electrode coverage was more limited. Moreover, inherent to the patient group undergoing intracranial EEG, the results are limited by the use of participants with epilepsy. While we aimed to limit this confound by eliminating data with subclinical or clinical epileptic activity, the networks investigated may be permanently altered by epilepsy and its comorbidities, limiting generalization to the healthy nervous system. However, the correspondence between the current results and previous investigations in healthy normal human and non-human subjects tempers this concern. It is possible that anticipatory activity or expectation of the next stimulus might have contributed to early signals close to stimulus onset, although the temporal jitter used in the study design would tend to reduce the consistency of such signals. Another limitation is the inherent restriction of electrode coverage to cortical networks, whereas subcortical brain regions including the midbrain tectum as well as other brainstem, thalamic and striatal circuits may be quite important to perceptual signal detection and amplification (Li et al., 2021)(Asadollahi and Knudsen, 2016; Bollimunta et al., 2018; Knudsen, 2011; Knudsen et al., 2017; Schiff et al., 2013; Van der Werf et al., 2002). Although non-human animal model studies can investigate these subcortical networks most directly, future human studies may also provide insights through increasing availability of subcortical depth electrodes used for therapeutic interventions (Fisher et al., 2010; Kronemer et al., 2021; Velasco et al., 2007). In this study, structural MRI was used to map electrode contact localizations for each participant to an average brain surface, however there are important advantages to localizing brain function in individuals (Laumann et al., 2015). The observed changes in gamma power could be related to individual folding patterns in future work to more accurately localize function to the brain surface. Finally, future studies should investigate gamma power synchronization and other inter-

actions across cortical regions in the early visual detection network (Rohenkohl et al., 2018).

4.4. Conclusion

Signal detection is the process of rapidly identifying incoming sensory inputs for additional attention amplification, processing, and encoding. Likewise, signal detection may be the first stage for stimuli to be realized in conscious experience (Blumenfeld, 2021). In a large dataset of intracranial EEG among participants completing a visual presentation and recall task, we observed a network of cortical regions involved at the earliest stages within 0–50 ms after stimulus onset suggesting a role in detection. These early regions included the caudal middle/frontal eye fields, orbital frontal, ventral medial/frontopolar cortex, visual processing cortex, and medial temporal parahippocampal cortex. Other regions, involved at later times included broad left hemisphere language networks related to subsequent recall of verbal stimuli, suggesting a separate role from early detection areas. Together, we show that visual stimulus detection and encoding is a staged process occurring over 100 s of milliseconds that involves many distributed anterior and posterior cortical structures beginning very early after stimulus onset.

Declaration of Competing Interest

The authors declare no conflict of interest.

Credit authorship contribution statement

Hunki Kwon: Resources, Formal analysis, Writing – original draft. **Sharif I. Kronemer:** Formal analysis, Writing – original draft. **Kate L. Christison-Lagay:** Formal analysis, Writing – original draft. **Aya Khalaf:** Formal analysis, Writing – original draft. **Jiajia Li:** Formal analysis, Writing – original draft. **Julia Z Ding:** Formal analysis, Writing – original draft. **Noah C Freedman:** Formal analysis, Writing – original draft. **Hal Blumenfeld:** Resources, Formal analysis, Writing – original draft.

Acknowledgements

This work was supported by the Betsy and Jonathan Blattmachr Family and by the Loughridge Williams Foundation. We are grateful to the patients who participated in this study enabling the RAM electrophysiology data set to be created. We also thank Michael J. Kahana for important initial discussions about this study, and are grateful to him and his team of investigators at the University of Pennsylvania Computational Memory Lab for curating the data and making it publicly available.

Data and code availability statement

All data used for the present investigation are from the free-recall task in the RAM project and are publicly available from http://memory.psych.upenn.edu/Data_Request. All code for the analysis used in this study as described in the Methods are openly available through https://github.com/BlumenfeldLab/Kwon-et-al_2021.

Supplementary materials

Supplementary material associated with this article can be found, in the online version, at doi:10.1016/j.neuroimage.2021.118608.

References

Asadollahi, A., Knudsen, E.I., 2016. Spatially precise visual gain control mediated by a cholinergic circuit in the midbrain attention network. Nat. Commun. 7, 13472.
Bar, M., 2003. A cortical mechanism for triggering top-down facilitation in visual object recognition. J. Cogn. Neurosci. 15, 600–609.
Baroni, F., van Kempen, J., Kawasaki, H., Kovach, C.K., Oya, H., Howard, M.A., Adolphs, R., Tsuchiya, N., 2017. Intracranial markers of conscious face perception in humans. Neuroimage 162, 322–343.
Benjamin, C.F., Walshaw, P.D., Hale, K., Gaillard, W.D., Baxter, L.C., Berl, M.M., Polczynska, M., Noble, S., Alkawadri, R., Hirsch, L.J., Constable, R.T., Bookheimer, S.Y., 2017. Presurgical language fMRI: Mapping of six critical regions. Hum. Brain Mapp. 38, 4239–4255.
Bichot, N.P., Schall, J.D., 2002. Priming in macaque frontal cortex during popout visual search: feature-based facilitation and location-based inhibition of return. J. Neurosci. 22, 4675–4685.
Bisley, J.W., Goldberg, M.E., 2010. Attention, intention, and priority in the parietal lobe. Annu. Rev. Neurosci. 33, 1–21.
Blanke, O., Morand, S., Thut, G., Michel, C.M., Spinelli, L., Landis, T., Seeck, M., 1999. Visual activity in the human frontal eye field. Neuroreport 10, 925–930.
Blumenfeld, Hal, 2021. Brain Mechanisms of Conscious Awareness: Detect, Pulse, Switch, and Wave. The Neuroscientist In press.
Bollimunta, A., Bogadhi, A.R., Krauzlis, R.J., 2018. Comparing frontal eye field and superior colliculus contributions to covert spatial attention. Nat. Commun. 9, 3553.
Bruce, C.J., Goldberg, M.E., 1985. Primate frontal eye fields. I. Single neurons discharging before saccades. J. Neurophysiol. 53, 603–635.
Burke, J.F., Long, N.M., Zaghloul, K.A., Sharan, A.D., Sperling, M.R., Kahana, M.J., 2014. Human intracranial high-frequency activity maps episodic memory formation in space and time. Neuroimage (85 Pt 2) 834–843.
Burke, J.F., Zaghloul, K.A., Jacobs, J., Williams, R.B., Sperling, M.R., Sharan, A.D., Kahana, M.J., 2013. Synchronous and asynchronous theta and gamma activity during episodic memory formation. J. Neurosci. 33, 292–304.
Corbetta, M., Shulman, G.L., 2002. Control of goal-directed and stimulus-driven attention in the brain. Nat. Rev. Neurosci. 3, 201–215.
Critchley, M., 1962. Clinical investigation of disease of the parietal lobes of the brain. Med. Clin. North Am. 46, 837–857.
Dastjerdi, M., Foster, B.L., Nasrullah, S., Rauschecker, A.M., Dougherty, R.F., Townsend, J.D., Chang, C.T., Greicius, M.D., Menon, V., Kennedy, D.P., Parvizi, J., 2011. Differential electrophysiological response during rest, self-referential, and non–self-referential tasks in human posteromedial cortex. Proc. Natl. Acad. Sci. U. S. Am. 108, 3023–3028.
Deco, G., Lee, T.S., 2004. The role of early visual cortex in visual integration: a neural model of recurrent interaction. Eur. J. Neurosci. 20, 1089–1100.
Desimone, R., Duncan, J., 1995. Neural mechanisms of selective visual attention. Annu. Rev. Neurosci. 18, 193–222.
Dobs, K., Isik, L., Pantazis, D., Kanwisher, N., 2019. How face perception unfolds over time. Nat. Commun. 10, 1258.
Dosenbach, N.U., Fair, D.A., Miezin, F.M., Cohen, A.L., Wenger, K.K., Dosenbach, R.A., Fox, M.D., Snyder, A.Z., Vincent, J.L., Raichle, M.E., Schlaggar, B.L., Petersen, S.E., 2007. Distinct brain networks for adaptive and stable task control in humans. Proc. Natl. Acad. Sci. U. S. Am. 104, 11073–11078.
Duecker, F., Formisano, E., Sack, A.T., 2013. Hemispheric differences in the voluntary control of spatial attention: direct evidence for a right-hemispheric dominance within frontal cortex. J. Cogn. Neurosci. 25, 1332–1342.
Fisher, R., Salanova, V., Witt, T., Worth, R., Henry, T., Gross, R., Oommen, K., Osorio, I., Nazzaro, J., Labar, D., Kaplitt, M., Sperling, M., Sandok, E., Neal, J., Handforth, A., Stern, J., DeSalles, A., Chung, S., Shetter, A., Bergen, D., Bakay, R., Henderson, J., French, J., Baltuch, G., Rosenfeld, W., Youkilis, A., Marks, W., Garcia, P., Barbaro, N., Fountain, N., Bazil, C., Goodman, R., McKhann, G., Babu Krishnamurthy, K., Papavassiliou, S., Epstein, C., Pollard, J., Tonder, L., Grebin, J., Coffey, R., Graves, N.Group, S.S., 2010. Electrical stimulation of the anterior nucleus of thalamus for treatment of refractory epilepsy. Epilepsia 51, 899–908.
Fornaciai, M., Brannon, E.M., Woldorff, M.G., Park, J., 2017. Numerosity processing in early visual cortex. NeuroImage 157, 429–438.
Foster, B.L., Dastjerdi, M., Parvizi, J., 2012. Neural populations in human posteromedial cortex display opposing responses during memory and numerical processing. Proc. Natl. Acad. Sci. U. S. Am. 109, 15514–15519.
Foxe, J.J., Simpson, G.V., 2002. Flow of activation from V1 to frontal cortex in humans. A framework for defining "early" visual processing. Exp. Brain Res. 142, 139–150.
Gaillard, R., Dehaene, S., Adam, C., Clemenceau, S., Hasboun, D., Baulac, M., Cohen, L., Naccache, L., 2009. Converging intracranial markers of conscious access. PLoS Biol. 7, e61.
Gregoriou, G.G., Gotts, S.J., Zhou, H., Desimone, R., 2009. High-frequency, long-range coupling between prefrontal and visual cortex during attention. Science 324, 1207–1210.
Grosbras, M.H., Paus, T., 2002. Transcranial magnetic stimulation of the human frontal eye field: effects on visual perception and attention. J. Cogn. Neurosci. 14, 1109–1120.
Hassabis, D., Kumaran, D., Vann, S.D., Maguire, E.A., 2007. Patients with hippocampal amnesia cannot imagine new experiences. Proc. Natl. Acad. Sci. U. S. A. 104, 1726–1731.
Heinen, K., Feredoes, E., Weiskopf, N., Ruff, C.C., Driver, J., 2014. Direct evidence for attention-dependent influences of the frontal eye-fields on feature-responsive visual cortex. Cereb. Cortex 24, 2815–2821.
Herman, W.X., Smith, R.E., Kronemer, S.I., Watsky, R.E., Chen, W.C., Gober, L.M., Touloumes, G.J., Khosla, M., Raja, A., Horien, C.L., Morse, E.C., Botta, K.L., Hirsch, L.J., Alkawadri, R., Gerrard, J.L., Spencer, D.D., Blumenfeld, H., 2019. A Switch and Wave of Neuronal Activity in the Cerebral Cortex During the First Second of Conscious Perception. Cereb. Cortex 29, 461–474.
Howard, M.W., Kahana, M.J., 1999. Contextual variability and serial position effects in free recall. J. Exp. Psychol. Learn. Mem. Cogn. 25, 923–941.
Jerbi, K., Vidal, J.R., Ossandon, T., Dalal, S.S., Jung, J., Hoffmann, D., Minotti, L., Bertrand, O., Kahane, P., Lachaux, J.P., 2010. Exploring the electrophysiological correlates of the default-mode network with intracerebral EEG. Front. Syst. Neurosci. 4, 27.

Kinomura, S., Larsson, J., Gulyas, B., Roland, P.E., 1996. Activation by attention of the human reticular formation and thalamic intralaminar nuclei. Science 271, 512–515.
Kirchner, H., Barbeau, E.J., Thorpe, S.J., Regis, J., Liegeois-Chauvel, C., 2009. Ultra-rapid sensory responses in the human frontal eye field region. J. Neurosci. 29, 7599–7606.
Klein, A., Tourville, J., 2012. 101 labeled brain images and a consistent human cortical labeling protocol. Front. Neurosci. 6, 171.
Knudsen, E.I., 2011. Control from below: the role of a midbrain network in spatial attention. Eur. J. Neurosci. 33, 1961–1972.
Knudsen, E.I., Schwarz, J.S., Knudsen, P.F., Sridharan, D., 2017. Space-specific deficits in visual orientation discrimination caused by lesions in the midbrain stimulus selection network. Curr. Biol. 27, 2053–2064 e2055.
Konkel, A., Cohen, N.J., 2009. Relational memory and the hippocampus: representations and methods. Front. Neurosci. 3, 166–174.
Kronemer, S.I., Aksen, M., Ding, J., Ryu, J.H., Xin, Q., Ding, Z., Prince, J.S., Kwon, H., Khalaf, A., Forman, S., Jin, D., Wang, K., Chen, K., Hu, C., Agarwal, A., Sabirski, E., Wafa, S.A., Morgan, O., Wu, J., Christison-Lagay, K., Hasulak, N., Morrell, M., Urban, A., Constable, R.T., Pitts, M., Richardson, R.M., Crowley, M., Blumenfeld, H., 2021. Brain networks in human conscious visual perception. In review Submitted for publication.
Laumann, T.O., Gordon, E.M., Adeyemo, B., Snyder, A.Z., Joo, S.J., Chen, M.Y., Gilmore, A.W., McDermott, K.B., Nelson, S.M., Dosenbach, N.U., Schlaggar, B.L., Mumford, J.A., Poldrack, R.A., Petersen, S.E., 2015. Functional system and areal organization of a highly sampled individual human brain. Neuron 87, 657–670.
Li, J., Kronemer, S.I., Herman, W.X., Kwon, H., Ryu, J.H., Micek, C., Wu, Y., Gerrard, J., Spencer, D.D., Blumenfeld, H., 2019. Default mode and visual network activity in an attention task: direct measurement with intracranial EEG. Neuroimage 201, 116003.
Li, R., Ryu, J.H., Vincent, P., Springer, M., Kluger, D., Levinsohn, E.A., Chen, Y., Chen, H., Blumenfeld, H., 2021. A pulse of fMRI increases in subcortical arousal systems during transitions in attention. Neuroimage 232, 117873.
Libedinsky, C., Livingstone, M., 2011. Role of prefrontal cortex in conscious visual perception. J. Neurosci. 31, 64–69.
Long, N.M., Burke, J.F., Kahana, M.J., 2014. Subsequent memory effect in intracranial and scalp EEG. Neuroimage 84, 488–494.
Luders, H., Lesser, R.P., Hahn, J., Dinner, D.S., Morris, H.H., Wyllie, E., Godoy, J., 1991. Basal temporal language area. Brain 114 (Pt 2), 743–754.
Marshall, T.R., O'Shea, J., Jensen, O., Bergmann, T.O., 2015. Frontal eye fields control attentional modulation of alpha and gamma oscillations in contralateral occipitoparietal cortex. J. Neurosci. 35, 1638–1647.
Meador, K.J., Ray, P.G., Echauz, J.R., Loring, D.W., Vachtsevanos, G.J., 2002. Gamma coherence and conscious perception. Neurology 59, 847–854.
Meeren, H.K., Hadjikhani, N., Ahlfors, S.P., Hamalainen, M.S., de Gelder, B., 2008. Early category-specific cortical activation revealed by visual stimulus inversion. PLoS One 3, e3503.
Miller, K.J., Honey, C.J., Hermes, D., Rao, R.P., denNijs, M., Ojemann, J.G., 2014. Broadband changes in the cortical surface potential track activation of functionally diverse neuronal populations. Neuroimage (85 Pt 2) 711–720.
Miller, K.J., Weaver, K.E., Ojemann, J.G., 2009. Direct electrophysiological measurement of human default network areas. Proc. Natl. Acad. Sci. U. S. A. 106, 12174–12177.
Mormann, F., Kornblith, S., Quiroga, R.Q., Kraskov, A., Cerf, M., Fried, I., Koch, C., 2008. Latency and selectivity of single neurons indicate hierarchical processing in the human medial temporal lobe. J. Neurosci. 28, 8865–8872.
Muggleton, N.G., Juan, C.H., Cowey, A., Walsh, V., 2003. Human frontal eye fields and visual search. J. Neurophysiol. 89, 3340–3343.
Mukamel, R., Gelbard, H., Arieli, A., Hasson, U., Fried, I., Malach, R., 2005. Coupling between neuronal firing, field potentials, and fMRI in human auditory cortex. Science 309, 951–954. %U http://www.sciencemag.org/content/309/5736/5951.abstract .
N'Diaye, K., Ragot, R., Garnero, L., Pouthas, V., 2004. What is common to brain activity evoked by the perception of visual and auditory filled durations? A study with MEG and EEG co-recordings. Brain Res. Cogn. Brain Res. 21, 250–268.
O'Shea, J., Muggleton, N.G., Cowey, A., Walsh, V., 2004. Timing of target discrimination in human frontal eye fields. J. Cogn. Neurosci. 16, 1060–1067.
Ossandón, T., Jerbi, K., Vidal, J.R., Bayle, D.J., Henaff, M.A., Jung, J., Minotti, L., Bertrand, O., Kahane, P., Lachaux, J.P., 2011. Transient suppression of broadband gamma power in the default-mode network is correlated with task complexity and subject performance. J. Neurosci. 31, 14521–14530.
Palva, S., Linkenkaer-Hansen, K., Naatanen, R., Palva, J.M., 2005. Early neural correlates of conscious somatosensory perception. J. Neurosci. 25, 5248–5258.
Pennartz, C.M.A., Dora, S., Muckli, L., Lorteije, J.A.M., 2019. Towards a unified view on pathways and functions of neural recurrent processing. Trends Neurosci. 42, 589–603.
Petroni, F., Panzeri, S., Hilgetag, C.C., Kotter, R., Young, M.P., 2001. Simultaneity of responses in a hierarchical visual network. Neuroreport 12, 2753–2759.
Ramot, M., Fisch, L., Harel, M., Kipervasser, S., Andelman, F., Neufeld, M.Y., Kramer, U., Fried, I., Malach, R., 2012. A widely distributed spectral signature of task-negative electrocorticography responses revealed during a visuomotor task in the human cortex. J. Neurosci. 32, 10458–10469.
Rohenkohl, G., Bosman, C.A., Fries, P., 2018. Gamma synchronization between V1 and V4 improves behavioral performance. Neuron 100, 953–963 e953.
Saalmann, Y.B., Pigarev, I.N., Vidyasagar, T.R., 2007. Neural mechanisms of visual attention: how top-down feedback highlights relevant locations. Science 316, 1612–1615.
Schacter, D.L., Addis, D.R., Buckner, R.L., 2007. Remembering the past to imagine the future: the prospective brain. Nat. Rev. Neurosci. 8, 657–661.
Schaefer, A., Kong, R., Gordon, E.M., Laumann, T.O., Zuo, X.N., Holmes, A.J., Eickhoff, S.B., Yeo, B.T.T., 2018. Local-global parcellation of the human cerebral cortex from intrinsic functional connectivity MRI. Cereb. Cortex 28, 3095–3114.
Schall, J.D., 2002. The neural selection and control of saccades by the frontal eye field. Philos. Trans. R. Soc. Lond. Ser. B Biol. Sci. 357, 1073–1082.
Schall, J.D., Morel, A., King, D.J., Bullier, J., 1995. Topography of visual cortex connections with frontal eye field in macaque: convergence and segregation of processing streams. J. Neurosci. 15, 4464–4487.
Schiff, N.D., Shah, S.A., Hudson, A.E., Nauvel, T., Kalik, S.F., Purpura, K.P., 2013. Gating of attentional effort through the central thalamus. J. Neurophysiol. 109, 1152–1163.
Schmolesky, M.T., Wang, Y., Hanes, D.P., Thompson, K.G., Leutgeb, S., Schall, J.D., Leventhal, A.G., 1998. Signal timing across the macaque visual system. J. Neurophysiol. 79, 3272–3278.
Sederberg, P.B., Schulze-Bonhage, A., Madsen, J.R., Bromfield, E.B., McCarthy, D.C., Brandt, A., Tully, M.S., Kahana, M.J., 2007. Hippocampal and neocortical gamma oscillations predict memory formation in humans. Cereb. Cortex 17, 1190–1196.
Seeley, W.W., Menon, V., Schatzberg, A.F., Keller, J., Glover, G.H., Kenna, H., Reiss, A.L., Greicius, M.D., 2007. Dissociable intrinsic connectivity networks for salience processing and executive control. J. Neurosci. 27, 2349–2356.
Shigihara, Y., Hoshi, H., Zeki, S., 2016. Early visual cortical responses produced by checkerboard pattern stimulation. Neuroimage 134, 532–539.
Shulman, G.L., Pope, D.L., Astafiev, S.V., McAvoy, M.P., Snyder, A.Z., Corbetta, M., 2010. Right hemisphere dominance during spatial selective attention and target detection occurs outside the dorsal frontoparietal network. J. Neurosci. 30, 3640–3651.
Silvanto, J., Lavie, N., Walsh, V., 2006. Stimulation of the human frontal eye fields modulates sensitivity of extrastriate visual cortex. J. Neurophysiol. 96, 941–945.
Sommer, M.A., Wurtz, R.H., 2004. What the brain stem tells the frontal cortex. I. Oculomotor signals sent from superior colliculus to frontal eye field via mediodorsal thalamus. J. Neurophysiol. 91, 1381–1402.
Tehovnik, E.J., Sommer, M.A., Chou, I.H., Slocum, W.M., Schiller, P.H., 2000. Eye fields in the frontal lobes of primates. Brain Res. Brain Res. Rev. 32, 413–448.
Thompson, K.G., Schall, J.D., 1999. The detection of visual signals by macaque frontal eye field during masking. Nat. Neurosci. 2, 283–288.
Thompson, K.G., Schall, J.D., 2000. Antecedents and correlates of visual detection and awareness in macaque prefrontal cortex. Vision. Res. 40, 1523–1538.
Turk-Browne, N.B., Scholl, B.J., Chun, M.M., Johnson, M.K., 2009. Neural evidence of statistical learning: efficient detection of visual regularities without awareness. J. Cogn. Neurosci. 21, 1934–1945.
Van der Werf, Y.D., Witter, M.P., Groenewegen, H.J., 2002. The intralaminar and midline nuclei of the thalamus. Anatomical and functional evidence for participation in processes of arousal and awareness. Brain Res. Brain Res. Rev. 39, 107–140.
Velasco, F., Velasco, A.L., Velasco, M., Jimenez, F., Carrillo-Ruiz, J.D., Castro, G., 2007. Deep brain stimulation for treatment of the epilepsies: the centromedian thalamic target. Acta Neurochir. Suppl. 97, 337–342.
Vossel, S., Geng, J.J., Fink, G.R., 2014. Dorsal and ventral attention systems: distinct neural circuits but collaborative roles. Neuroscientist 20, 150–159.
Wang, S., Mamelak, A.N., Adolphs, R., Rutishauser, U., 2018. Encoding of target detection during visual search by single neurons in the human brain. Curr. Biol. 28, 2058–2069 e2054.